

The influence of displacement ventilation on indoor carbon dioxide exposure and ventilation efficiency in a living laboratory open-plan office

Yalin Lu^{a,b,c}, Junkai Huang^a, Danielle N. Wagner^{a,b}, Zhang Lin^d, Nusrat Jung^a, Brandon E. Boor^{a,b,*}

^a Lyles School of Civil Engineering, Purdue University, West Lafayette, IN, 47907, United States

^b Ray W. Herrick Laboratories, Center for High Performance Buildings, Purdue University, West Lafayette, IN, 47907, United States

^c Department of Civil, Environmental, and Architectural Engineering, Worcester Polytechnic Institute, Worcester, MA, 01609, United States

^d Department of Architecture and Civil Engineering, City University of Hong Kong, Hong Kong, China

ARTICLE INFO

Keywords:

Mechanical ventilation
Office air quality
Indoor air distribution
Exposure assessment
Occupancy

ABSTRACT

Good indoor air quality in office environments is essential for occupant health and productivity. In open-plan offices, displacement ventilation has been recognized for its higher efficiency compared to mixing ventilation. This study evaluates the performance of displacement ventilation in an open-plan office under cooling and heating conditions, considering various supply ventilation rates, supply air temperatures, and occupancy levels. Field measurements were conducted over three months in a living laboratory office in a high-performance building. The indoor environment was controlled by an independent variable air volume (VAV) air conditioning system. The supply ventilation rate ranged from 6 to 12 h⁻¹. Real-time measurements of carbon dioxide (CO₂) concentrations in the supply air, return air, and breathing zone of the office were conducted to assess occupants' exposure to CO₂ and ventilation efficiency. The results show that the supply ventilation rate plays an important role in shaping the air distribution and overall effectiveness of the mechanical ventilation system. Higher supply ventilation rates can enhance air distribution robustness, improving ventilation efficiency and reducing CO₂ exposure under both cooling and heating conditions. These findings also suggest the need for an optimized control logic that differs from the conventional control logic used in VAV systems. Specifically, during the heating condition of displacement ventilation, it is recommended to maintain the supply ventilation rate at a higher level to effectively mitigate the impact of occupant behavior on air quality, minimize CO₂ exposure risks, and ensure a more robust and reliable indoor air distribution.

1. Introduction

Elevated indoor exposure to air pollutants is associated with an increased incidence of sick building syndrome symptoms [1,2], significantly impacting the health and well-being of occupants. Among various indoor air pollutants, such as fine and coarse particulate matter [3,4], volatile organic compounds [5], and ozone [6,7], carbon dioxide (CO₂) is commonly monitored in commercial buildings as it provides information about ventilation efficiency and occupancy [8]. The American Society of Heating, Refrigerating, and Air-Conditioning Engineers (ASHRAE) has established ANSI/ASHRAE Standard 62.1–2022 [9], stipulating that the minimum outdoor volumetric airflow rate in the breathing zone should be 2.5 L/s-person plus 0.3 L/s-m² for office spaces. Furthermore, amid the COVID-19 pandemic, indoor CO₂ has

been utilized as a reliable proxy for airborne infection risk [10,11]. The Federation of European Heating, Ventilation, and Air Conditioning Associations (REHVA) has proposed an infection risk-based target ventilation rate for open-plan offices ranging from 16.5 to 25.4 L/s-person, depending on ventilation effectiveness. This results in indoor CO₂ concentrations of 619–736 ppm [12,13]. Given the crucial role of effective mechanical ventilation in commercial buildings for mitigating the airborne transmission of respiratory viruses, CO₂ has become an important parameter for understanding the influence of indoor air distribution on occupants' exposure to exhaled bioeffluents [14] and ventilation efficiency. Burrige et al. [15] established a model to infer airborne infection risk by monitoring indoor CO₂ concentrations. They demonstrated the effectiveness of using CO₂ concentrations to predict airborne infection in both mechanically and naturally ventilated offices.

* Corresponding author. Lyles School of Civil Engineering, Purdue University, West Lafayette, IN, 47907, United States.

E-mail address: bboor@purdue.edu (B.E. Boor).

<https://doi.org/10.1016/j.buildenv.2024.111468>

Received 22 November 2023; Received in revised form 22 February 2024; Accepted 26 March 2024

Available online 29 March 2024

0360-1323/© 2024 Elsevier Ltd. All rights reserved.

Fantozzi et al. [16] proposed an operating principle, monitoring CO₂ concentrations to control infection probability below a critical value for naturally ventilated classrooms. These studies emphasized the significance of real-time CO₂ data as a key indicator in assessing the risk of airborne infections. Park and Song [17] established CO₂ concentration thresholds for controlling airborne transmission of SARS-CoV-2 under different air exchange rates, occupancy levels, and exposure times. These studies assume that the indoor air is well-mixed in ventilated rooms and show that increasing air exchange rates reduce CO₂ concentrations proportionally. This observation holds true for idealized mixing ventilation. However, for many advanced room air distribution systems with non-uniform air distribution [18], the dynamics can differ significantly.

Typically, ventilation efficiency indicators are employed to evaluate the extent of non-uniformity in room air distributions. Tian et al. [19] conducted experiments to measure the contaminant removal effectiveness (CRE) of different air distribution systems with contaminant sources at the floor and armpit levels. Their findings revealed that for mixing ventilation, the CRE ranged from 0.63 to 1.07, displacement ventilation showed a range of 0.91–1.71, and stratum ventilation exhibited a range of 0.84–1.49. In another study, Yamasawa et al. [20] compared the CRE of impinging jet ventilation and displacement ventilation, demonstrating that displacement ventilation achieved higher CRE values, ranging from 1.42 to 1.83, compared with impinging jet ventilation with a range of 1.04–1.49. CRE is widely used to assess indoor air quality. It indicates the location of the contaminant source relative to the indoor air distribution. A CRE between zero and unity suggests the contaminant source is in the recirculation area. A CRE equal to unity signifies well-mixed room air, where the contaminant source position has no effect on the concentration distribution. A CRE higher than unity indicates that the source is near the outlet [21–23]. For airborne infection control, where infections are primarily caused by the inhalation of infectious aerosol [24], greater emphasis should be placed on air quality in the breathing zone rather than the location of the contaminant source. As different ventilation indicators are defined for different purposes [25], in this study, we use the air utilization effectiveness (AUE) metric to assess room air distribution. The AUE indicates the efficiency of using filtered supply air to clean the breathing zone [26].

Displacement ventilation is widely used in office buildings [27]. It supplies air slightly lower than the room temperature setting to occupants from diffusers located along the lower part of the walls [28]. As the air rises after being heated by indoor heat sources, such as occupants, displacement ventilation achieves an upward unidirectional airflow that effectively removes exhaled contaminants, thus improving ventilation efficiency [29]. While displacement ventilation is not intended for room heating due to the buoyancy of heated air disrupting the unidirectional airflow, it can be used for heating with the proper design considerations, e.g., through combination with a separate heating system like a radiator, radiant floor, or fan coil unit [28,30,31], or pre-heating the space during unoccupied periods [32].

Under cooling conditions, the boundary layer of an occupant can entrain the clean air from areas lower than the breathing zone to reduce personal exposure to bioeffluents [33], but it can be disturbed by occupant movement [34], the supply ventilation rate [35–37], and respiratory airflows [38]. Wu and Lin [39,40] compared the effect of a walking occupant on different ventilation conditions, and the indoor airflow under displacement ventilation is more susceptible to the influence of occupant movement. Licina et al. [36,37] found that increased horizontal air velocity can influence the occupant's convective boundary layer and result in increased exposure to pollutants. Yang et al. [35] investigated the influence of the ventilation rate on the CO₂ concentration in the breathing zone and global mean CO₂ concentration under displacement ventilation, showing that an excessively high supply ventilation rate can cause the air to bypass the breathing zone, resulting in increased exposure to exhaled CO₂.

Under heating conditions, the unidirectional airflow is disturbed,

which might lead to decreased indoor air quality. Besides the supply air temperature, other factors may also influence indoor air quality under displacement ventilation. Yamasawa et al. [41] experimentally investigated the heating performance of displacement ventilation. The authors found that with a small supply ventilation rate, the heated air rises before it enters the occupied zone, causing contaminants to stagnate in the middle level of the room. However, with a large supply volumetric airflow rate, displacement ventilation still outperforms mixing ventilation with respect to indoor air quality.

Existing studies of laboratory-based experiments involving manikins [20,29,33,36–41] and computational fluid dynamics (CFD) simulations [34,35] provide valuable insight into the indoor air quality characteristics of displacement ventilation. However, these studies were conducted in well-controlled or static conditions and cannot accurately replicate real-world scenarios, particularly for a variety of occupant behaviors that are challenging to quantify. These behaviors greatly influence room air and contaminant distributions, as well as room load, which, in turn, affects the HVAC system's response and operation. Therefore, it is crucial to conduct field measurements in environments where occupants are non-static and their behaviors are uncontrolled. This approach allows us to capture the actual operational situations more accurately.

This study aims to investigate the influence of displacement ventilation on indoor CO₂ exposure and ventilation efficiency under realistic mechanical ventilation conditions in an occupied open-plan office, utilizing occupant-generated CO₂ as a tracer gas [42] to examine the room air distribution. A field measurement campaign was conducted in one of the four living laboratory offices at the Purdue University Ray W. Herrick Laboratories under variable occupancy and supply air conditions (ventilation rate, temperature, heating vs. cooling). The living laboratory offices are part of a modern high-performance building. The building was designed and constructed following criteria for future high-performance buildings and includes a state-of-the-art building automation and sensing platform and energy-efficient heating, ventilation, and air conditioning (HVAC) technologies. The office was occupied by graduate students who did not follow any specific work schedules and worked flexible hours. The office featured an independently controlled displacement ventilation system that included a variable air volume (VAV) system. CO₂ concentrations were measured at multiple locations throughout the office and its HVAC system, including at breathing zone height, via a multi-location sampling platform. The results of the study are used to provide operational suggestions for implementing displacement ventilation with a VAV system in office environments.

2. Materials and methods

2.1. Experimental setup

2.1.1. Site description: Herrick living laboratory open-plan offices at Purdue University

The living laboratory open-plan office has dimensions of 10.5 m (length) × 9.9 m (width) × 3.2 m (height) [7]. Fig. 1 shows the layout of the office, and Fig. 2 presents photos of the office. The office has a maximum seating capacity of 20 people and contains 20 assigned desks and chairs arranged as a grid of 4 rows with 5 desks each (Fig. 1). Observations indicated the occupants remained seated, aside from brief periods of standing entry and exit and group discussions.

The office includes its own HVAC system that is monitored and controlled through a building automation system enabled by Tridium JACE controllers and the Niagara/AX software framework (Tridium Inc., Richmond, VA, U.S.A.). The HVAC system is modular in design and can be configured to simulate various mechanical ventilation conditions, including passive chilled beams [43], mixing ventilation, and displacement ventilation, among others. For the measurement campaign, the HVAC system was configured with a combined displacement ventilation and VAV system. As illustrated in Fig. 2, the ventilation configuration

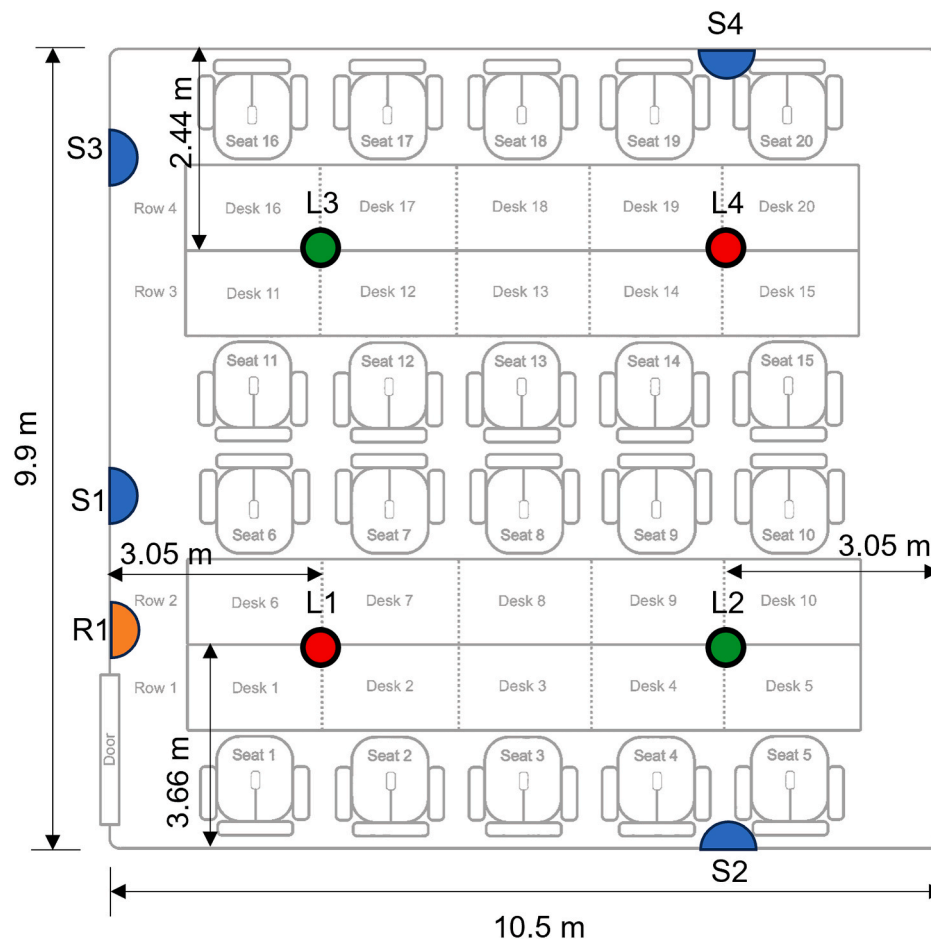


Fig. 1. Schematic of the living laboratory office, supply diffuser locations (S1 to S4), return air louver location (R1), and measurement locations for seated occupancy and breathing zone (L1 to L4) CO₂ concentrations (adapted from Ref. [44]).

included four displacement diffusers positioned at the four corners of the office and one return air louver located near the ceiling on the left-hand side wall. The supply ventilation rate was regulated at three stages, approximately 6, 9, and 12 h⁻¹ (equivalent to 5.3, 8.0, and 10.7 L/s·m² or 27.7, 41.6, and 55.4 L/s·person), with these values monitored and controlled by the Niagara/AX control platform. In displacement ventilation, maintaining a design air temperature difference between foot and head levels of less than 2 °C is essential to prevent discomfort [30]. Consequently, the required supply ventilation rate is approximately 6 h⁻¹ for a temperature difference of 2 °C and 12 h⁻¹ for a temperature difference of 1 °C. During the measurements, the room air temperature setpoint was kept at a constant 21.9 °C via the Niagara/AX control platform. The air handling unit supplies air with a temperature of 12.8 °C to the VAV box. When the room air temperature falls below the setpoint temperature, the control platform maintains the room air temperature by increasing the heating hot water valve opening and reducing the damper opening of the VAV box to supply warm air, and at the same time adjusting the supply ventilation rate to 6 h⁻¹. When the room air temperature exceeds the setpoint temperature, the control platform maintains the room air temperature by decreasing the heating hot water valve opening and increasing the damper opening of the VAV box to adjust the supply air temperature and supply ventilation rate to the room.

2.1.2. Multi-location measurements of occupancy, CO₂ concentrations, and air temperatures

Office seated occupancy was measured with 60 s time-resolution via a chair-based temperature sensor array. Each chair is equipped with a K-

type epoxy coated tip thermocouple (TC-PVC-K-24-180, Omega Engineering Inc., Norwalk, CT, U.S.A.) connected to a battery-powered datalogger (EasyLog EL-USB-TC, Lascar Electronics Inc., Erie, PA, U.S.A.) to detect seated occupancy for each of the 20 desk-chair pairs in the office (Figs. 1 and 2). The thermocouple was positioned at the middle of the upward-facing seat cushion and attached to the cushion with double-sided fabric tape. The data analysis approach used to determine the seated occupancy is described in detail by Wagner et al. [44]. In brief, a chair is considered occupied when the seat surface temperature exceeds a threshold value. Periodic observations of seated occupants were performed throughout the campaign to validate the output of the chair-based temperature sensor array.

A multi-location sampling system was used to measure CO₂ concentrations (as mixing ratios, ppm) and dry bulb air temperatures at various locations throughout the living laboratory office and its HVAC system. Table 1 presents the measured locations and parameters. Locations L1 to L4 in Table 1 correspond to the labeled positions shown in Fig. 1. CO₂ concentrations were measured through a combination of two measurement approaches (Fig. 3). For the first approach, CO₂ concentrations were measured with a laboratory-grade non-dispersive infrared (NDIR) CO₂ gas analyzer (LI-830, LICOR Biosciences, Lincoln, NE, U.S.A.) with a range of 0–20,000 ppm and accuracy of <3 % of the reading. The LI-830 was calibrated at the beginning of the measurement campaign using pure CO₂ gas diluted by ultra-zero air. The LI-830 was connected to an automated indoor air sampling system (Fig. 3a) to measure the CO₂ concentration at six different locations, including four locations in the breathing zone of the seated occupants (Fig. 3b), one in the return air duct (Fig. 3c), and one in the supply air duct (Fig. 3d). A

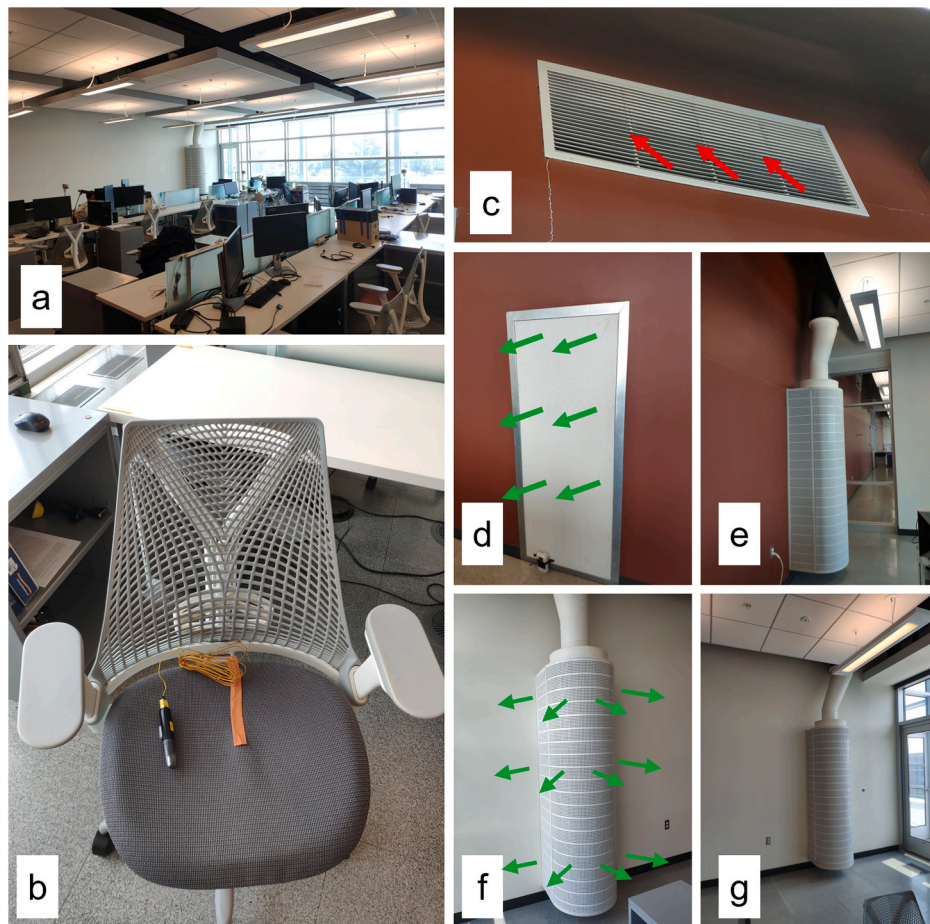


Fig. 2. Photos of the living laboratory office: (a) overview, (b) chair with K-type thermocouple and data logger, (c) return air louver near ceiling, and (d) to (g) supply diffusers; arrows indicate airflow directions.

Table 1
Measured locations and parameters.

Location	Air Temperature	CO ₂ Concentration
L1-1.5 m	✓	
L1-1.1 m	✓	
L2-1.5 m	✓	✓
L2-1.1 m	✓	✓
L3-1.5 m	✓	✓
L3-1.1 m	✓	✓
L4-1.5 m	✓	
L4-1.1 m	✓	
Supply Air Duct	✓	✓
Return Air Duct	✓	✓

‘common-outlet’ type, programmable multi-port valve (EUTA-2VLS8MWE2, Valco Instruments Co. Inc., Houston, TX, U.S.A.) was used to sequentially regulate the sample air from eight different locations for delivery to the LI-830 (Fig. 3e and f) with a cycle duration of 120 s.

While the indoor CO₂ monitoring with the LI-830 provided an accurate assessment of the spatial variation in CO₂ concentrations within the living laboratory office and its HVAC system, the measurements were not made concurrently due to the timing of the valve sequence. To provide the additional concurrent measurement of CO₂ concentrations, the second approach utilized an array of portable battery-powered NDIR CO₂ loggers (HOBO MX 1102A, Onset Computer Corp., Bourne, MA, U.S.A.). The CO₂ sensors have a range of 0–5000 ppm and an accuracy of 50 ppm. To evaluate the accuracy of the CO₂ sensors, they were compared against the LI-830 during co-location measurements. An example is

shown in Fig. 4, where both the HOBO MX 1102A and LI-830 measured CO₂ concentrations in the seated breathing zone for one day during the measurement campaign. The mean absolute error (MAE) for the HOBO MX 1102A ranged from 23.43 to 27.80 ppm, with larger errors observed during the periodic spikes in indoor CO₂ concentrations. However, the overall trend monitored by the HOBO MX 1102A agreed well with the LI-830. In addition to CO₂, the HOBO MX 1102A measured air temperatures at each location with a range of 0–50 °C and an accuracy of ±0.21 °C. Table 2 provides a summary of the measurement instrumentation.

2.1.3. Experimental protocol

The participants in this study were the existing occupants of the living laboratory office. During the measurement campaign, no personal information was requested from the participants, and we did not interfere with their presence or activities. The measurements were conducted between February and April 2023, with data collected during normal occupied periods from 10:00 to 17:00. The CO₂ concentrations, air temperatures, supply ventilation rates, and seated occupancy were recorded during this period. The temperature in the occupied zone as measured with the HOBO MX 1102A sensors remained stable within the range of 22.1–24.6 °C, which is higher than the temperature setpoint of 21.9 °C. This can be attributed to the placement of the thermostat for the Niagara/AX control platform, which is on the sidewall of the office instead of the occupied zone.

To collect data on the displacement ventilation system operating under various supply air conditions (specifically, supply ventilation rates of 6, 9, and 12 h⁻¹, with the room undergoing heating and cooling), the control platform was overridden during the measurement

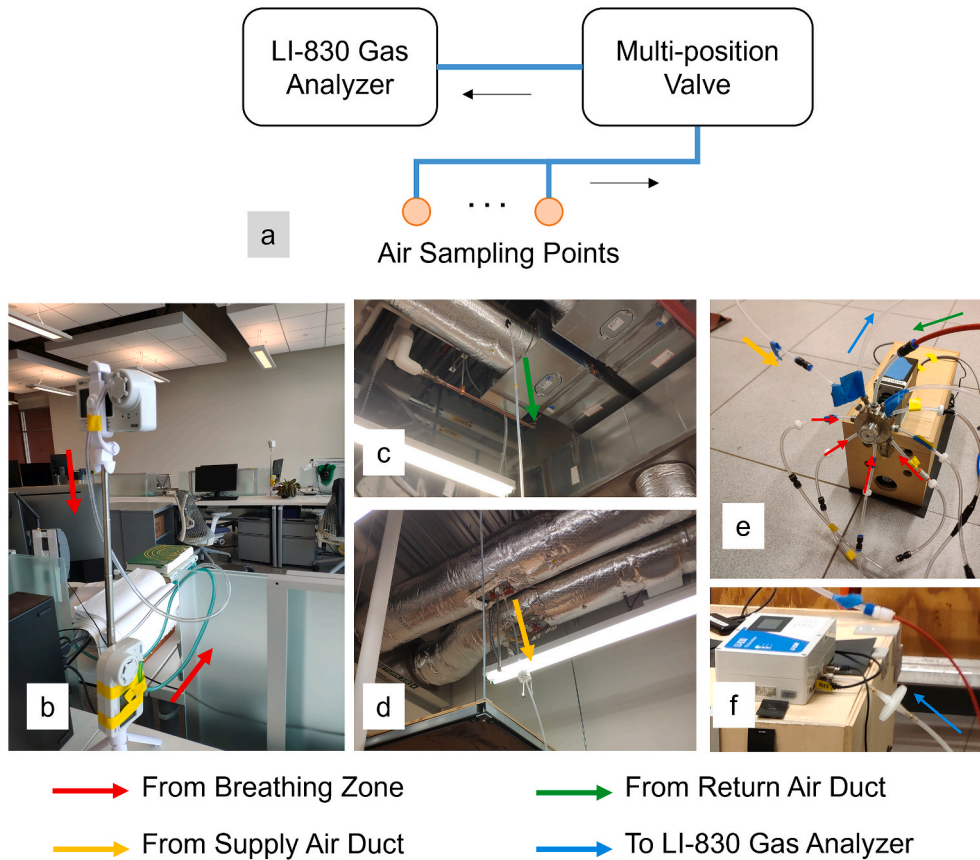


Fig. 3. (a) Schematic of the air sampling system for multi-location CO₂ measurements in the living laboratory office and its HVAC system, (b) sampling locations in the breathing zone, (c) sampling location from the return air duct, (d) sampling location from the supply air duct, (e) sampled air to the multi-position valve, (f) sampled air to the LI-830 CO₂ gas analyzer.

campaign, with minimal adjustments made. Table 3 summarizes the supply air conditions. In Condition 1, the VAV system operated under default settings with the maximum supply ventilation rate set to 12 h⁻¹ for cooling and the supply ventilation rate under heating at 6 h⁻¹, with the maximum opening of the heating hot water valve set to 100%. In Condition 2, only the maximum supply ventilation rate for cooling was adjusted to 9 h⁻¹, and in Condition 3, it was adjusted to 6 h⁻¹. Throughout these three conditions, the VAV system alternately supplied cool and warm air to maintain the room temperature at the set point. Due to the time lag in the supply air temperature during the transition from heating mode to cooling mode, there were instances when the supply ventilation rate changed to 9 or 12 h⁻¹, yet warm air continued to be supplied to the space. In Condition 4, an all-day cooling operation was desired, so the maximum opening of the heating hot water valve was limited to 50% based on the condition established in Condition 3. This limitation aimed to prevent the VAV system from supplying air warmer than the temperature setpoint to the office space.

2.2. Evaluation metrics

2.2.1. Exposure to indoor CO₂ concentrations

The elevation in the CO₂ concentration measured at the various breathing zone locations beyond that measured in the supply air duct was used to evaluate occupant exposure to exhaled CO₂ under various displacement ventilation conditions. This approach allows for a closer examination of the impact of occupant behavior on the indoor air distribution. This measurement campaign was conducted without modifying occupant behavior in the office, thereby allowing for various occupant behaviors that could potentially influence the CO₂ distribution in the office. It is important to note that the occupancy, supply

ventilation rate, and other factors, such as the location and movement of occupants within the office, can influence the observed CO₂ distribution. The sensitivity of the air distribution to occupant behaviors under different supply ventilation rates can be visualized and assessed using box plots [45] of CO₂ concentrations, which provides insights into the robustness of different air distributions.

2.2.2. Ventilation efficiency

The air utilization effectiveness (AUE) metric is employed to evaluate the ventilation efficiency of the indoor air distribution under different supply ventilation rates and heating/cooling conditions for the displacement ventilation system of the living laboratory office. As the supply ventilation rate and supply air temperature impact the indoor air distribution, the AUE can be used to describe the air distribution and indicate its effectiveness. The AUE value ranges from $-\infty$ to unity. An AUE equal to unity indicates that the air distribution is comparable to personalized ventilation, where clean air is directly supplied to the occupants' breathing zone. An AUE equal to zero indicates an idealized mixing ventilation, and an AUE less than zero indicates that the breathing zone is in the recirculation zone of the air distribution. Moreover, the AUE demonstrates good linearity with the airborne infection risk for respiratory viruses; a higher AUE value indicates a lower airborne infection risk [26]. The AUE is calculated as follows:

$$AUE = \frac{C_r - C_b}{C_r - C_s} \quad (1)$$

where C_r is the CO₂ concentration (ppm) measured in the return air duct of the displacement ventilation system; C_b is the CO₂ concentration (ppm) measured in the breathing zone of the seated office occupants; and C_s is the CO₂ concentration (ppm) measured in the supply air duct of

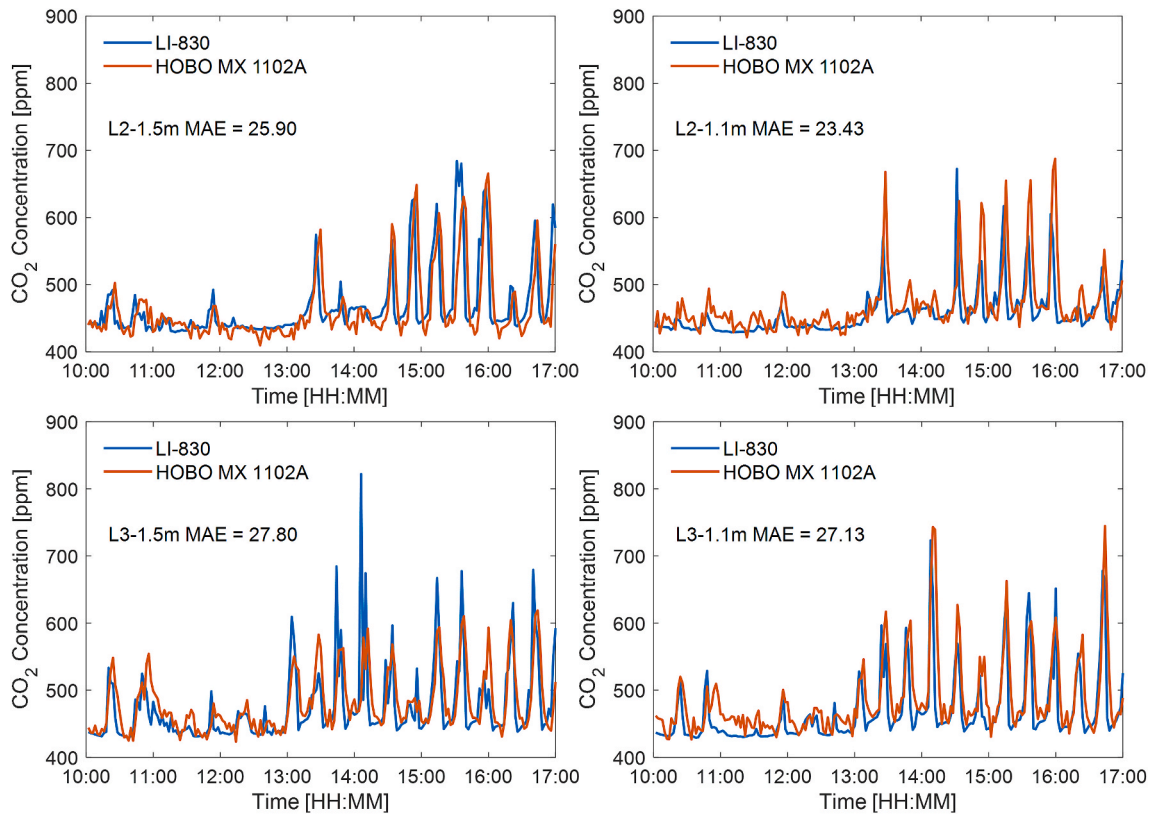


Fig. 4. Co-location measurements of breathing zone CO₂ concentrations in the living laboratory office as measured by the LI-830 CO₂ gas analyzer and HOBO MX 1102A CO₂ sensor.

Table 2
Summary of measurement instrumentation.

Instrument	Parameter	Range	Sampling Interval	Accuracy	Resolution	Application
LI-830 (LICOR Biosciences, Lincoln, NE, U.S.A.)	CO ₂	0 to 20,000 ppm	0.5 s	<3% of the reading	0.31 ppm	To measure indoor CO ₂ concentrations at different locations.
Temperature datalogger (EasyLog EL-USB-TC, Lascar Electronics Inc., Erie, PA, U.S.A.) with K-type epoxy coated tip thermocouple (TC-PVC-K-24-180, Omega Engineering Inc., Norwalk, CT, U.S.A.)	Temperature	0 to 200 °C	60 s	±1 °C	0.5 °C	To measure the surface temperature of office chairs to detect seated occupancy.
CO ₂ logger (HOBO MX 1102A, Onset Computer Corp., Bourne, MA, U.S.A.)	CO ₂	0 to 5,000 ppm	60 s	±5% of the reading at 25 °C	1 ppm	To provide additional concurrent measurement of CO ₂ concentrations at different locations.
	Temperature	0 to 50 °C	60 s	±0.21 °C from 0 to 50 °C	0.024 °C at 25 °C	To measure air temperature at different locations.
Multi-port valve (EUTA-2VLS8MWE2, Valco Instruments Co. Inc., Houston, TX, U.S.A.)	–	–	15 s	–	–	To sequentially regulate the sample air from different locations for delivery to the LI-830.

Table 3
VAV system operation conditions.

VAV Operation Condition	Maximum Supply Ventilation Rate for Cooling (h ⁻¹)	Supply Ventilation Rate for Heating (h ⁻¹)	Maximum Heating Hot Water Valve Opening
Condition 1 (default)	12	6	100%
Condition 2	9	6	100%
Condition 3	6	6	100%
Condition 4	6	6	50%

the displacement ventilation system.

2.2.3. Energy efficiency

The energy-efficient operation of an air distribution system is always of interest. In this study, the energy performance of the non-uniform air distribution is assessed using the thermal utilization effectiveness (TUE). The TUE is defined as the ratio of the temperature difference between the air at the return duct and in the occupied zone to the difference between the air at the return and supply ducts, as shown in Equation (2) [46].

$$TUE = \frac{T_r - T_o}{T_r - T_s} \quad (2)$$

where T_r is the air temperature ($^{\circ}\text{C}$) measured in the return air duct of the displacement ventilation system; T_o is the air temperature ($^{\circ}\text{C}$) measured in the occupied zone of the seated office occupants; and T_s is the air temperature ($^{\circ}\text{C}$) measured in the supply air duct of the displacement ventilation system.

Therefore, TUE can evaluate the relative contribution of occupied zones to the energy performance of the air distribution system. For instance, if T_o approaches T_s , TUE will be unity, signifying that the conditioned air is ideally utilized for the thermal conditions of the occupied zone. Typically, ideal personalized ventilation achieves a TUE of unity. In contrast, if T_o is identical to T_r , TUE will be zero, indicating ideal mixing ventilation. A negative TUE value implies that the supply air is short-circuited to the occupied zone.

3. Results and discussion

3.1. Temporal variations in the supply ventilation rate, air temperatures, and CO₂ concentrations in the living laboratory office under displacement ventilation

Fig. 5 illustrates time-dependent changes in the supply ventilation rate, air temperatures, and CO₂ concentrations throughout the day under each of the four displacement ventilation conditions in the living laboratory office. Under Condition 1 with the default setting (Fig. 5a), the VAV system operated alternately between cooling and heating

modes, with the supply ventilation rate ranging from 6 to 12 h^{-1} . As a result, the office space experienced alternating heating and cooling cycles to maintain the room air temperature stable at the setpoint from 10:00 to 14:40. Subsequently, it continued to supply cool air to the office space with a ventilation rate of 6 h^{-1} . The CO₂ concentration measured in both the return air duct and breathing zone exhibited transient fluctuations, with the concentration in the breathing zone fluctuating more, sometimes exceeding 100 ppm compared with the supply air concentration. This led to fluctuations in the AUE throughout the day. Under Condition 2, the supply ventilation rate ranged from 6 to 9 h^{-1} , and the supply air temperature and CO₂ concentrations fluctuated similarly to Condition 1 (Fig. 5b). The highest CO₂ concentrations measured in the breathing zone were about 200 ppm greater than those measured in the supply air duct. For Conditions 3 and 4 (Fig. 5c and d), the supply ventilation rate was stabilized at 6 h^{-1} .

In Condition 3, the office space experienced alternating cycles of warm and cool air supply, causing the CO₂ concentration in the breathing zone to fluctuate with the change of the supply air temperature, with peaks nearly 150 ppm higher than the supply air concentration (Fig. 5c). Under Condition 4, where the supply air temperature never exceeded the breathing zone temperature, the CO₂ concentration in the breathing zone remained consistently low, under 20 ppm higher than the supply air (Fig. 5d). Comparing Conditions 3 and 4, it can be concluded that the temporal fluctuations in CO₂ concentrations in the breathing zone are mainly caused by changes in the supply air

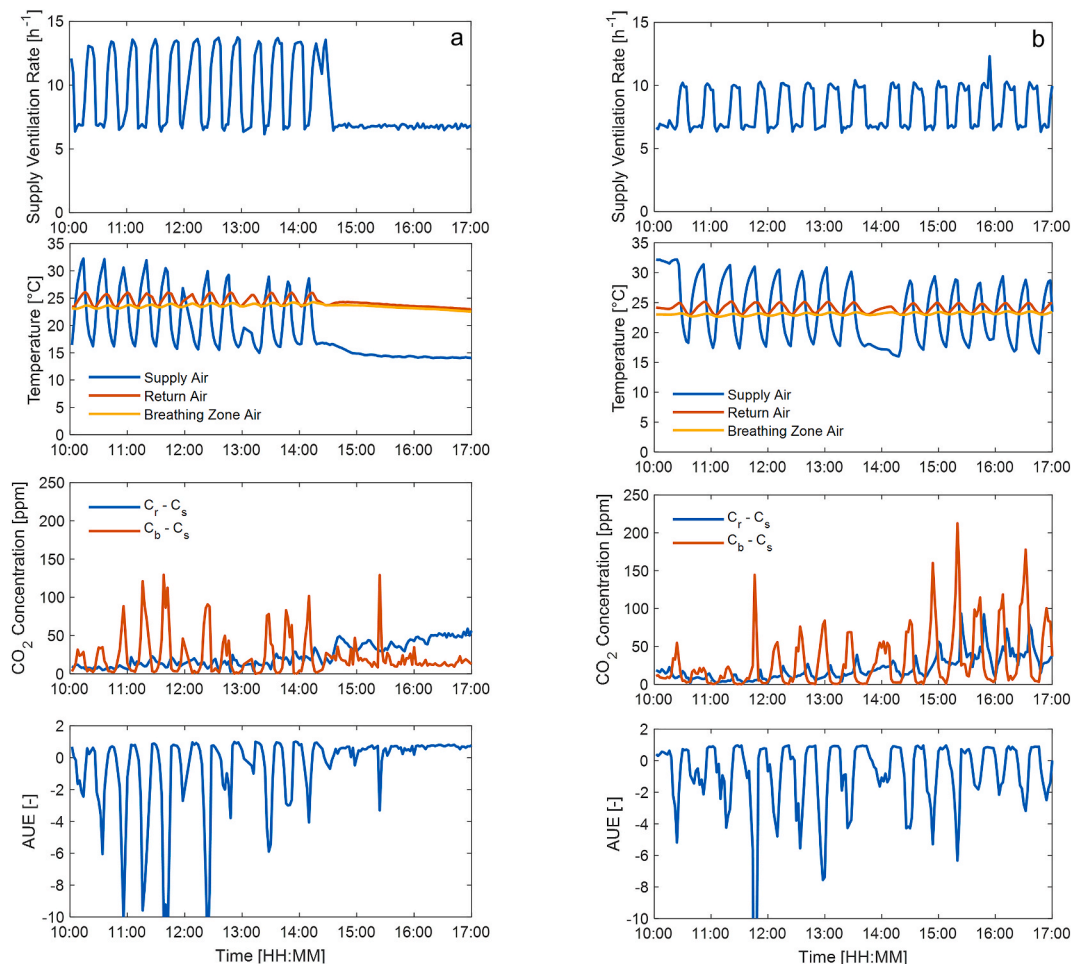


Fig. 5. Time-dependent changes in the supply ventilation rate; temperatures as measured in the supply air duct, return air duct, and breathing zone; CO₂ concentrations as measured in the return air duct and breathing zone (minus that in the supply air duct); and the air utilization effectiveness (AUE) under displacement ventilation conditions with a nominal supply ventilation rate of 6 h^{-1} for the living laboratory office: (a) Condition 1 (default setting), (b) Condition 2, (c) Condition 3, and (d) Condition 4.

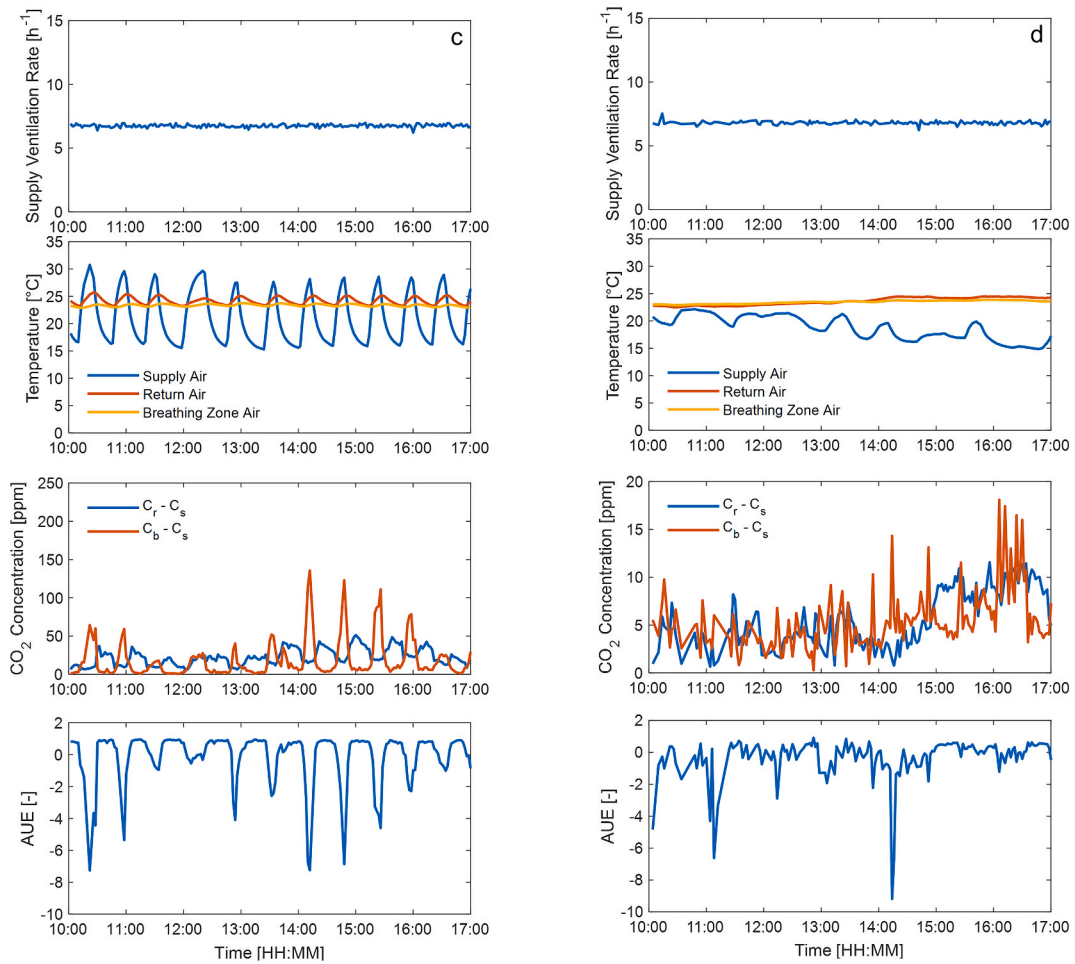


Fig. 5. (continued).

temperature. When warm air is supplied to the office space, the air distribution is affected by the warm supply air, causing a spike in CO_2 concentration in the breathing zone. In Condition 3, the AUE approaches

unity, while in Condition 4, the maximum AUE is approximately zero. This indicates that the smaller air temperature difference between the supply air and breathing zone in Condition 4 impairs the directional

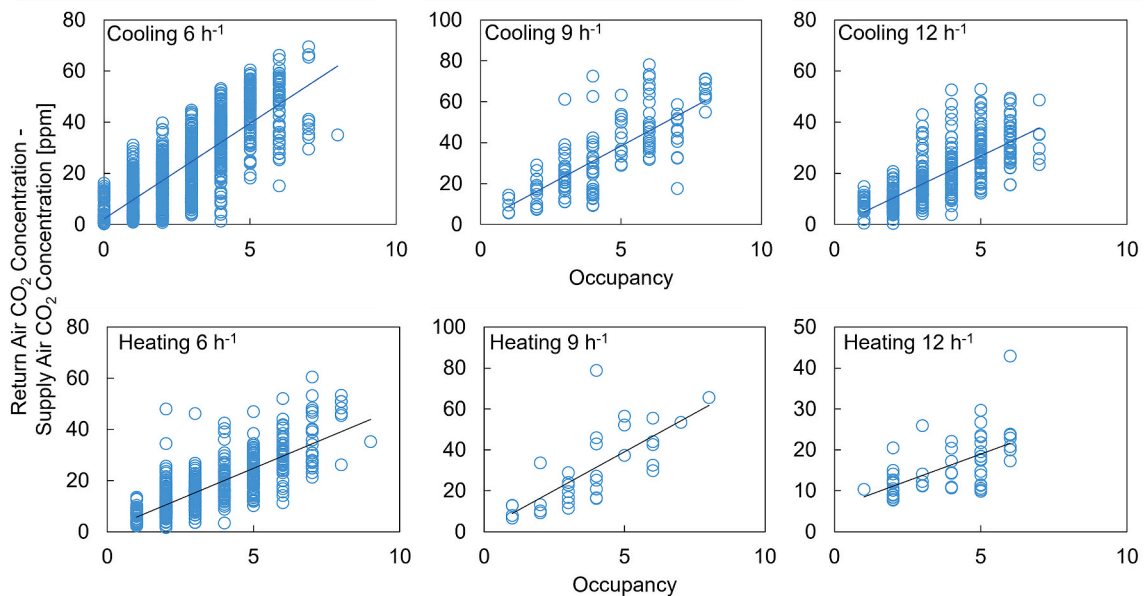


Fig. 6. CO_2 concentrations as measured in the return air duct (minus that in the supply air duct) vs. occupancy under different displacement ventilation conditions for the living laboratory office.

airflow of displacement ventilation, making the ventilation efficiency comparable to that of mixing ventilation [47].

Displacement ventilation demonstrates effective performance in maintaining indoor air quality under cooling conditions, consistent with findings from prior studies on displacement ventilation [19,20,48]. While there has been no specific field investigation into using displacement ventilation exclusively for room heating, given that its primary purpose is not to supply warm air, such scenarios can occur in practice. For instance, in the living laboratory office examined in this study, the use of displacement ventilation for heating was associated with elevated CO₂ exposure and reduced ventilation efficiency.

3.2. Influence of office occupancy and supply ventilation rate on return air and breathing zone CO₂ concentrations in the living laboratory office under displacement ventilation

Fig. 6 illustrates the relationship between the CO₂ concentration measured in the return air duct (minus that measured in the supply air duct: $C_r - C_s$) of the living laboratory office and the seated occupancy, showing a positive correlation. The linearity of this relationship is further supported by the data presented in Table 4. Under the cooling condition of the displacement ventilation system, the slopes range from 5.45 to 7.47 for different supply ventilation rates (h^{-1}), with Pearson correlation coefficients ranging from 0.74 to 0.79. Under the heating condition of the displacement ventilation system, the slopes are 2.63–7.54 for different supply ventilation rates, with Pearson correlation coefficients ranging from 0.60 to 0.79.

The slope provides insights into the removal performance of occupant exhaled CO₂ in the living laboratory office. The slope would decrease with an increased supply ventilation rate under a well-mixed indoor air distribution. This is because a higher return volumetric airflow rate leads to a lower CO₂ concentration in the return air, assuming a constant CO₂ mass flow rate leaving the office. However, the measurement results deviate from this expectation in that the ventilation efficiency improves proportionally with the increase of supply ventilation rate [48], indicating a non-uniform indoor air distribution under displacement ventilation for both cooling and heating conditions. Under the cooling condition, the slope is slightly higher at a supply ventilation rate of 6 h^{-1} (7.47) compared to that at 9 h^{-1} (7.40), indicating a poorer performance in CO₂ removal when the supply ventilation rate decreases to 6 h^{-1} . Under the heating condition, the slopes at 6 and 12 h^{-1} are approximately half of those observed under the cooling condition. However, at 9 h^{-1} , the slope remains similar (cooling: 7.40, heating: 7.54), suggesting a similar efficiency in exhaled CO₂ removal from the office, which implies that under 6 and 12 h^{-1} , the efficiency of CO₂ removal is more sensitive to the supply air temperature.

Fig. 7 illustrates the relationship between the mean CO₂ concentration measured across the various breathing zone locations (minus that measured in the supply air duct: $C_b - C_s$) of the living laboratory office and the seated occupancy, also showing a positive correlation for the various displacement ventilation conditions. The linearity of this relationship is further supported by the data presented in Table 5. Under the cooling condition, the slopes range from 1.98 to 3.62 for different supply

Table 4
Summary of return air CO₂ concentration and occupancy correlation analysis.

HVAC Condition	Supply Ventilation Rate (h^{-1})	Pearson Correlation Coefficient	Slope	Number of Data Points
Cooling	6	0.79	7.47	1288
	9	0.74	7.40	125
	12	0.74	5.45	386
Heating	6	0.79	4.78	565
	9	0.74	7.54	32
	12	0.60	2.63	53

ventilation rates, with Pearson correlation coefficients ranging from 0.36 to 0.54. Under the heating condition, the slopes range from 2.81 to 15.12 for different supply ventilation rates, with Pearson correlation coefficients ranging from 0.36 to 0.65. The CO₂ concentration measured in the breathing zone can show a significant discrepancy compared to that measured in the return air under displacement ventilation, primarily due to the non-uniform air distribution [14,49,50].

The slope of the relationship between office seated occupancy and CO₂ exposure as measured at breathing zone height (1.1 and 1.5 m) provides insights into the indoor air quality in the office. The slope decreases as the supply airflow ventilation increases (from 3.62 at 6 h^{-1} to 1.98 at 12 h^{-1}), indicating that higher supply air volumetric airflow rates result in lower CO₂ exposure levels for occupants and improved indoor air quality. However, under the heating condition, the slopes under 6 h^{-1} (15.12) and 9 h^{-1} (10.89) are significantly higher than that under 12 h^{-1} (2.81) and under the cooling conditions (1.98–3.62), suggesting a higher CO₂ concentration in the breathing zone and less optimal indoor air quality in the living laboratory office. These findings show the significant influence of the supply air temperature on indoor airflow patterns in occupied open-plan offices when using displacement ventilation systems with wall-mounted supply diffusers. Maintaining good indoor air quality is achievable with supply ventilation rates ranging from 6 to 12 h^{-1} during cooling periods. This is because, under cooling conditions, the higher density of the cooled supply air causes it to flow downward, resulting in lower air temperatures near the floor compared to the upper room. Around the occupants, the cooled air flows upward, interacting with the thermal plume generated by occupants and effectively removing CO₂ in the occupied zone. However, the indoor air distribution in the office under displacement ventilation becomes highly sensitive to the supply ventilation rate during heating periods. This sensitivity arises due to the absence of the unidirectional airflow characteristic of displacement ventilation when the supply ventilation rate is set at 6 and 9 h^{-1} . In this scenario, the lower density of the heated air causes it to flow upward after being discharged. When the velocity of the supply air is low, it can ascend without passing through the occupant zone, resulting in the accumulation of CO₂ in the occupied zone.

More sampling points were taken at 6 h^{-1} for heating and cooling due to various factors. In Supply Air Conditions 1 and 2, we set limitations on the maximum supply ventilation rate. The actual supply ventilation rate for cooling is dependent on the room load, with low occupancy most of the time, resulting in a predominantly 6 h^{-1} supply ventilation rate. However, for Conditions 3 and 4, the cooling supply ventilation rate was consistently fixed at 6 h^{-1} . Regarding heating, the displacement ventilation operated exclusively at 6 h^{-1} . The operation under 9 and 12 h^{-1} is attributed to the thermal inertia of the VAV box during the transition from heating to cooling, as explained in Section 2.1.3. Recognizing the potential impact of the higher number of sampling points at 6 h^{-1} compared to the other two supply ventilation rates, we conducted separate analyses for each supply ventilation rate. This approach provides a comprehensive understanding of displacement ventilation under various operational conditions.

Fig. 8 shows the range in the measured CO₂ concentrations at different breathing zone heights (1.1 and 1.5 m) under different displacement ventilation conditions (minus that measured in the supply air duct: $C_b - C_s$). Thus, the results indicate the localized elevations in CO₂ exposure beyond the background levels in the office as measured in the supply air duct. Under each displacement ventilation condition, the mean CO₂ concentration at a breathing zone height of 1.5 m is 28–74 % higher than that at a breathing zone height of 1.1 m under cooling conditions and 31–65 % higher under heating conditions, which is consistent with indoor contaminant stratification [20,47,51] for displacement ventilation. This is because the exhaled air has a higher temperature than the room air, allowing the exhaled CO₂ from the seated occupants to flow vertically upwards.

The measured CO₂ concentrations at both breathing zone heights are significantly higher under the heating condition (~10–100 ppm beyond

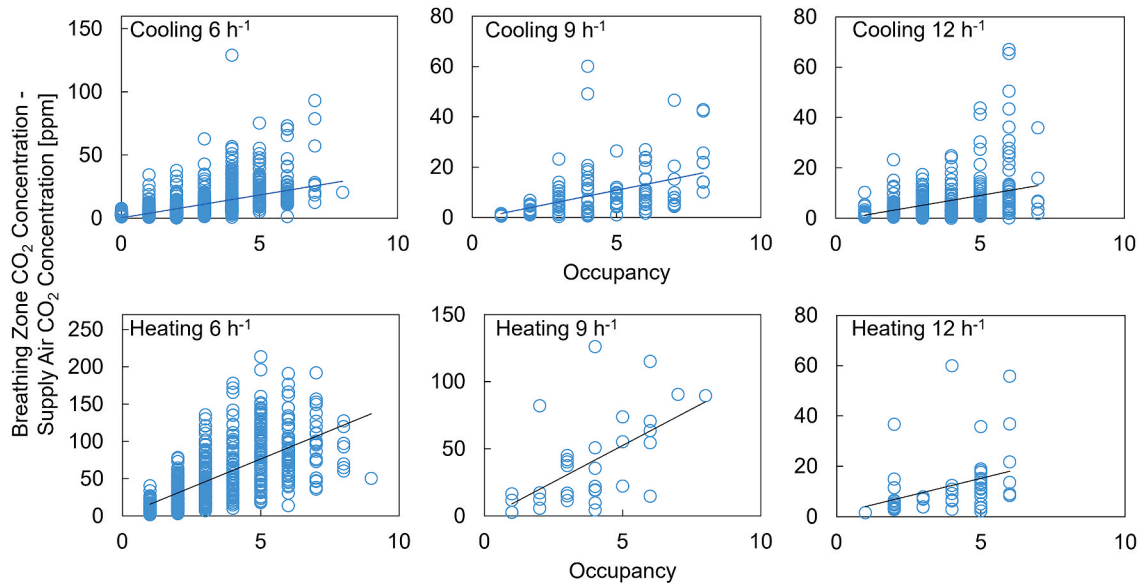


Fig. 7. CO₂ concentrations as measured in the breathing zone (minus that in the supply air duct) vs. occupancy under different displacement ventilation conditions for the living laboratory office.

Table 5
Summary of breathing zone CO₂ concentration and occupancy correlation analysis.

HVAC Condition	Supply Ventilation Rate (h ⁻¹)	Pearson Correlation Coefficient	Slope	Number of Data Points
Cooling	6	0.54	3.62	1288
	9	0.41	2.32	125
	12	0.36	1.98	386
Heating	6	0.65	15.12	565
	9	0.59	10.89	32
	12	0.36	2.81	53

condition, the supply air has a temperature higher than the room air, which leads to the clean air flowing upwards from the displacement diffusers without passing through the breathing zone of the occupants. With the supply ventilation rate increasing from 6 to 9 h⁻¹, the supply air velocity increases, and more clean air enters the occupied zone before flowing upwards. Therefore, the CO₂ concentration in the breathing zone is slightly lower under 9 h⁻¹, with the mean CO₂ concentration in the breathing zone being 26 % lower than that under 6 h⁻¹. As the supply ventilation rate increases to 12 h⁻¹, the CO₂ concentration in the breathing zone decreases significantly, with the mean CO₂ concentration in the breathing zone being 78 % lower than that under 6 h⁻¹. This indicates that filtered supply air effectively enters the breathing zone with the increased supply air velocity.

supply air) than in the cooling condition (~1–10 ppm beyond supply air). Under the cooling condition, supply air with a temperature lower than the room air enters the occupied zone and the exhaled CO₂ is driven by buoyancy to the upper zone of the office. Under the heating

3.3. Sensitivity in breathing zone CO₂ concentrations to occupant behavior

Assuming that occupant behavior remained consistent throughout

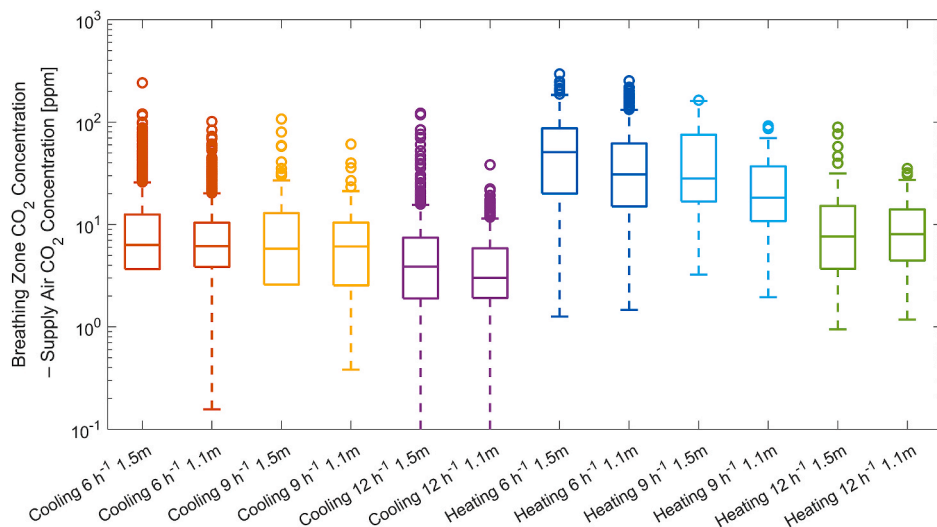


Fig. 8. CO₂ concentrations measured at different breathing zone heights (1.1 and 1.5 m) under different displacement ventilation conditions for the living laboratory office.

the duration of the measurement campaign in the living laboratory office, Fig. 8 provides insights into the sensitivity of the indoor CO₂ distribution to occupant behavior. Under the cooling condition of the displacement ventilation system, the mean breathing zone CO₂ concentrations range from 4.56 to 11.15 ppm, with outliers mostly below 100 ppm, showing that the indoor air distribution remains relatively resilient to changes in the supply ventilation rate and occupant behavior (occupancy patterns and movement). However, under the heating condition, the mean breathing zone CO₂ concentrations range from 10.23 to 60.10 ppm, and outliers can reach as high as 150–300 ppm at a supply ventilation rate of 6 h⁻¹. These outliers can be attributed to occupant movements that introduce a mixing effect [29,39,52]. Such disturbances result in abrupt increases in CO₂ levels since the filtered supply air is unable to reach the breathing zone with the unidirectional airflow. With an increase in the supply ventilation rate to 12 h⁻¹, extremely high CO₂ concentrations were not observed. This is because the increased air velocity can increase the robustness [53,54] of the air distribution. Consequently, the indoor air distribution becomes less susceptible to variations in occupant behavior.

3.4. Influence of displacement ventilation conditions on ventilation efficiency

Fig. 9 shows the ventilation efficiency as assessed by the AUE metric under various displacement ventilation conditions in the living laboratory office. Under the cooling condition, the AUE values are consistently close to unity from 6 to 12 h⁻¹ and across all supply air temperatures (~13–23 °C). This indicates that the indoor air distribution achieved by displacement ventilation is comparable to personalized ventilation. This finding is also supported by the low CO₂ concentrations observed in the breathing zone, as illustrated in Figs. 6 and 7. However, there are instances where the AUE is lower than zero, potentially due to occupant movement within the office leading to short-term elevations in breathing zone concentrations beyond that in the return air ($C_b > C_r$).

Under the heating condition of the displacement ventilation system, a decreasing trend in the AUE is observed as the supply air temperature increases from ~23 to 32 °C and when the supply ventilation rate is 6 and 9 h⁻¹. This indicates that more supply air bypasses the breathing zone at a higher supply air temperature. For a supply ventilation rate of 12 h⁻¹, the AUE remains relatively stable with the increase in the supply air temperature from ~23 to 30 °C. As a low AUE indicates that the performance of the indoor air distribution is poor in mitigating airborne infection risks, utilizing a low supply ventilation rate under heating could increase the potential airborne infection risk in the office.

3.5. Influence of displacement ventilation conditions on energy efficiency

Fig. 10 shows the energy efficiency of various displacement ventilation scenarios evaluated by the TUE metric. In cooling conditions across all supply air temperatures (~13–23 °C), there is an increasing

trend in TUE values with the rise of the supply air temperature. This trend suggests that maintaining a supply air temperature slightly lower than the occupant zone temperature is close to the ideal personalized ventilation, where conditioned air effectively reaches the occupied zones. Conversely, supplying air with a much lower temperature than the occupied zone leads to downward airflow, expending more energy on conditioning the lower part of the room rather than the occupied zones. Comparing TUE fluctuations around zero for 6 and 12 h⁻¹, it is observed that under 9 h⁻¹, TUE remains stable at zero and above. Considering occupants as internal heat sources influencing local air distribution, displacement ventilation under 6 h⁻¹ can be easily disturbed by the thermal plume of occupants, resulting in locally mixed, even short-circuited supply airflow, leading to TUE values near zero or negative. At 12 h⁻¹, the local air movement due to displacement ventilation is stronger than the thermal plume of occupants, resulting in locally mixed air movement and TUE values close to zero. At a supply ventilation rate of 9 h⁻¹, there is a balance between the thermal plume and local air movement, allowing the supply air not to be disturbed by the thermal plume and maintaining TUE values at zero and above. Under heating conditions in the displacement ventilation system, TUE values are consistently less than zero across all supply air temperatures (~23–32 °C), indicating continuous short-circuiting of the air distribution.

3.6. Discussion

The results derived from the multi-location CO₂ measurements conducted under various displacement ventilation conditions within the living laboratory office offer valuable insights, allowing for the formulation of design and control strategies. Displacement ventilation demonstrates the potential to reduce CO₂ exposure during cooling periods. However, careful operation is essential during the heating period, as highlighted by the findings in Fig. 9. The presented results emphasize the importance of maintaining a high supply ventilation rate, specifically at 9 h⁻¹ during cooling conditions and 12 h⁻¹ for heating conditions for this office, to ensure minimal CO₂ exposure. This contrasts with the conventional control logic of a VAV system, which typically uses a minimum supply ventilation rate during the heating period. Therefore, an approach beyond conventional control strategies is warranted when designing ventilation systems to minimize exposure and associated airborne infection risks, all while considering energy efficiency. In this study, our discussion is centered on the energy performance of the room-side air distribution, as depicted in Fig. 10. The energy consumption of the entire HVAC system, including components like the fan and pump, was not the primary focus. For a more comprehensive understanding of energy consumption aspects, additional details can be explored in Ref. [43].

In this study, our focus was on personal exposure, also referred to as the personal CO₂ cloud [55] or personal CO₂ bubble [56], and ventilation measures to control exposure levels. High exposure can be

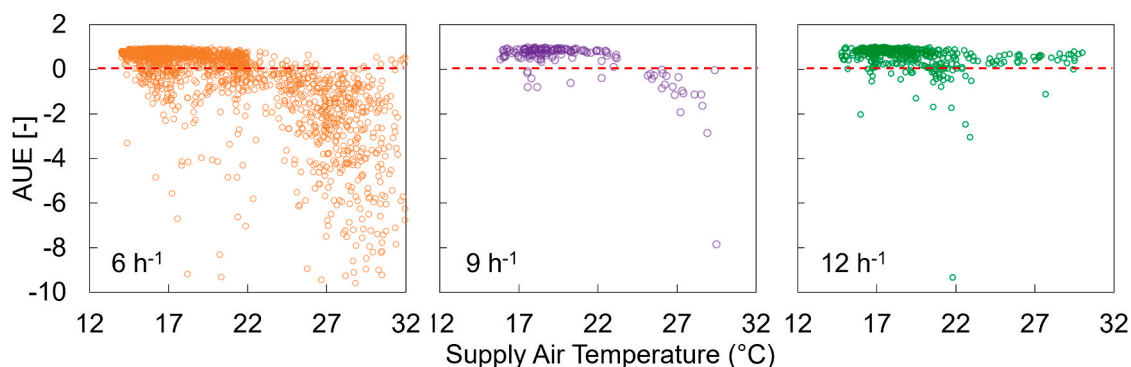


Fig. 9. Air utilization effectiveness (AUE) under different displacement ventilation conditions for the living laboratory office.

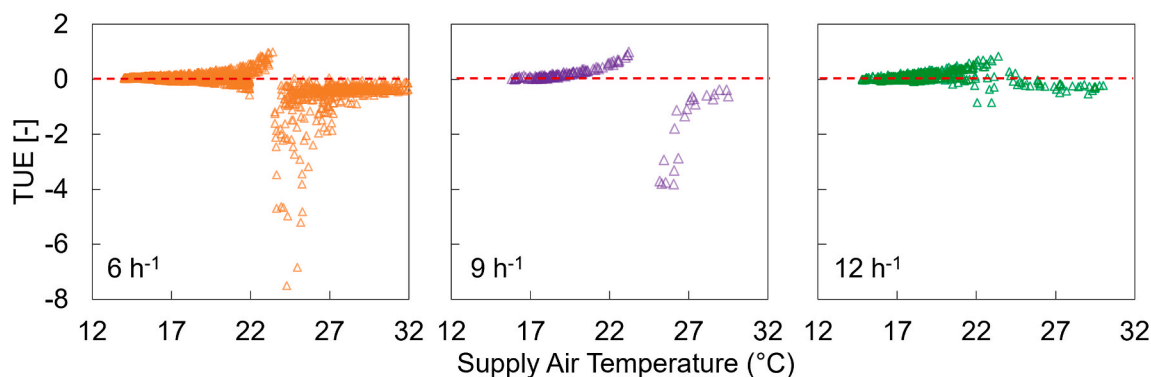


Fig. 10. Temperature utilization effectiveness (TUE) under different displacement ventilation conditions for the living laboratory office.

attributed to low local air velocity and increasing the supply ventilation rate can mitigate this by enhancing the local air movement. Some specific occupant behaviors affect personal exposures, such as using a desk fan [56], which can increase the local air velocity from 0.1 to 0.5 m/s. Our results, as shown in Figs. 6 and 7, indicate that the return air CO₂ concentration can underestimate personal exposure to CO₂. This finding is consistent with those in Ref. [55], emphasizing the importance of monitoring breathing zone CO₂ for effective control of ventilation systems.

While the measurement campaign in the living laboratory had a relatively low occupancy, representing less than 50% of the maximum room capacity, the findings can still provide insights into the performance of the displacement ventilation system. The scalability of results to full occupancy scenarios can be justified, as contaminant removal in displacement ventilation is primarily driven by the thermal plume of each occupant. Therefore, the observed trends and system behavior under low occupancy conditions can be indicative of how the system might perform in situations with higher occupant density. However, the experiment was conducted between February and April 2023, and the influence of the building envelope on indoor air distribution may vary across different seasons. This seasonal variability will be taken into account in future research. Lastly, only one human bioeffluent (CO₂) was measured at different locations throughout the office and its HVAC system. Thus, the impact of displacement ventilation conditions on spatial variations in concentrations of other species that are present in exhaled breath (e.g., respiratory aerosol, volatile organic compounds) was not evaluated.

4. Conclusions

This study investigated the influence of the supply ventilation rate, supply air temperature, and occupancy on the indoor CO₂ concentration distribution and ventilation efficiency under a displacement ventilation system for a living laboratory office. The findings demonstrate that the supply ventilation rate plays a critical role in shaping the indoor air distribution and overall effectiveness of displacement ventilation for an occupied open-plan office. Under both cooling and heating conditions, higher supply ventilation rates (9 and 12 h⁻¹) were found to enhance the robustness of the room air distribution, leading to improved ventilation efficiency and lower CO₂ concentrations in the breathing zone. Furthermore, a high supply ventilation rate can effectively mitigate the impact of occupant behavior on office air quality, reducing the probability of high exposure to exhaled CO₂ and ensuring a healthier indoor environment.

These findings have significant implications for the design and operation of displacement ventilation systems, especially for heating conditions. Engineers and designers should carefully match the supply ventilation rate and temperature to ensure adequate air is delivered to the breathing zone, thereby minimizing exhaled CO₂ exposure risks and

achieving optimal ventilation efficiency.

CRediT authorship contribution statement

Yalin Lu: Writing – review & editing, Writing – original draft, Visualization, Validation, Resources, Methodology, Investigation, Funding acquisition, Formal analysis, Data curation, Conceptualization. **Junkai Huang:** Writing – review & editing, Methodology, Investigation, Data curation. **Danielle N. Wagner:** Writing – review & editing, Methodology, Investigation, Data curation. **Zhang Lin:** Writing – review & editing, Supervision, Resources, Methodology, Investigation, Funding acquisition, Conceptualization. **Nusrat Jung:** Writing – review & editing, Supervision, Resources, Project administration, Methodology, Investigation, Data curation, Conceptualization. **Brandon E. Boor:** Writing – review & editing, Visualization, Validation, Supervision, Software, Resources, Project administration, Methodology, Investigation, Funding acquisition, Formal analysis, Data curation, Conceptualization.

Declaration of competing interest

The authors declare that they have no conflict of interest.

Data availability

Data will be made available on request.

Acknowledgments

The work described in this paper is supported by a General Research Grant from the Research Grants Council of the Hong Kong Special Administrative Region, China (Project No. CityU 11217722) and the National Science Foundation (CBET-1847493 to B.E.B.). The authors thank Dr. Jie Ma, Dr. Haotian Liu, Jinglin Jiang, Chunxu Huang, Ashley Ancil, and Dean Smoll for their assistance during the measurement campaign.

References

- [1] J. Hou, et al., Associations of indoor carbon dioxide concentrations, air temperature, and humidity with perceived air quality and sick building syndrome symptoms in Chinese homes, *Indoor Air* 31 (4) (2021) 1018–1028, <https://doi.org/10.1111/ina.12810>.
- [2] M.G. Apte, W.J. Fisk, J.M. Daisey, *Associations between Indoor CO₂ Concentrations and Sick Building Syndrome Symptoms in US Office Buildings: an Analysis of the 1994-1996 BASE Study Data, 2000*.
- [3] D.N. Wagner, S.R. Odhiambo, R.M. Ayikukwei, B.E. Boor, High time-resolution measurements of ultrafine and fine woodsmoke aerosol number and surface area concentrations in biomass burning kitchens: a case study in Western Kenya, *Indoor Air* 32 (10) (2022), <https://doi.org/10.1111/ina.13132>.
- [4] J. Jiang, N. Jung, B.E. Boor, Using building energy and smart thermostat data to evaluate indoor ultrafine particle source and loss processes in a net-zero energy

- house, ACS ES&T Engineering 1 (4) (2021) 780–793, <https://doi.org/10.1021/acsestengg.1c00002>.
- [5] J. Jiang, et al., Ethanol-based disinfectant sprays drive rapid changes in the chemical composition of indoor air in residential buildings, J Hazard Mater Lett 2 (2021) 100042, <https://doi.org/10.1016/j.hazl.2021.100042>.
- [6] J. Jiang, et al., Real-time measurements of botanical disinfectant emissions, transformations, and multiphase inhalation exposures in buildings, Environ. Sci. Technol. Lett. 8 (7) (2021) 558–566, <https://doi.org/10.1021/acs.estlett.1c00390>.
- [7] T. Wu, A. Tasoglou, H. Huber, P.S. Stevens, B.E. Boor, Influence of mechanical ventilation systems and human occupancy on time-resolved source rates of volatile skin oil ozonolysis products in a LEED-certified office building, Environ. Sci. Technol. 55 (24) (2021) 16477–16488, <https://doi.org/10.1021/acs.est.1c03112>.
- [8] H. Rahman, H. Han, Bayesian estimation of occupancy distribution in a multi-room office building based on CO₂ concentrations, Build. Simulat. 11 (3) (2017) 575–583, <https://doi.org/10.1007/s12273-017-0413-9>.
- [9] Ventilation For Acceptable Indoor Air Quality, ANSI/ASHRAE Standard 62.1-2022, ASHRAE, 2022.
- [10] Y. Lu, et al., Affordable measures to monitor and alarm nosocomial SARS-CoV-2 infection due to poor ventilation, Indoor Air (2021), <https://doi.org/10.1111/ina.12899>.
- [11] Z. Peng, J.L. Jimenez, Exhaled CO₂ as a COVID-19 infection risk proxy for different indoor environments and activities, Environ. Sci. Technol. Lett. 8 (5) (2021) 392–397, <https://doi.org/10.1021/acs.estlett.1c00183>.
- [12] J. Kurnitski, et al., Post-COVID ventilation design: infection risk-based target ventilation rates and point source ventilation effectiveness, Energy Build. 296 (2023), <https://doi.org/10.1016/j.enbuild.2023.113386>.
- [13] N.V. Group, Health-based Target Ventilation Rates and Design Method for Reducing Exposure to Airborne Respiratory Infectious Diseases. REHVA Proposal for Post COVID Target Ventilation Rates, 2022.
- [14] S. Yun, D. Licina, Optimal sensor placement for personal inhalation exposure detection in static and dynamic office environments, Build. Environ. 241 (2023), <https://doi.org/10.1016/j.buildenv.2023.110459>.
- [15] H.C. Burridge, S. Fan, R.L. Jones, C.J. Noakes, P.F. Linden, Predictive and retrospective modelling of airborne infection risk using monitored carbon dioxide, Indoor Built Environ. 31 (5) (2021) 1363–1380, <https://doi.org/10.1177/1420326x211043564>.
- [16] F. Fantozzi, G. Lamberti, F. Leccese, G. Salvadori, Monitoring CO₂ concentration to control the infection probability due to airborne transmission in naturally ventilated university classrooms, Architect. Sci. Rev. 65 (4) (2022) 306–318, <https://doi.org/10.1080/00038628.2022.2080637>.
- [17] S. Park, D. Song, CO₂ concentration as an indicator of indoor ventilation performance to control airborne transmission of SARS-CoV-2, Journal of Infection and Public Health 16 (7) (2023) 1037–1044, <https://doi.org/10.1016/j.jiph.2023.05.011>.
- [18] B. Yang, et al., A review of advanced air distribution methods - theory, practice, limitations and solutions, Energy Build. 202 (2019), <https://doi.org/10.1016/j.enbuild.2019.109359>.
- [19] X. Tian, B. Li, Y. Ma, D. Liu, Y. Li, Y. Cheng, Experimental study of local thermal comfort and ventilation performance for mixing, displacement and stratum ventilation in an office, Sustain. Cities Soc. 50 (2019), <https://doi.org/10.1016/j.scs.2019.101630>.
- [20] H. Yamasawa, T. Kobayashi, T. Yamanaka, N. Choi, M. Matsuzaki, Experimental investigation of difference in indoor environment using impinging jet ventilation and displacement ventilation systems, Int. J. Vent. 21 (3) (2021) 229–246, <https://doi.org/10.1080/14733315.2020.1864572>.
- [21] A. Novoselac, J. Srebric, Comparison of air exchange efficiency and contaminant removal effectiveness as IAQ indices, Build. Eng. 109 (2) (2003) 11.
- [22] C. Zhang, M. Pomianowski, P.K. Heiselberg, T. Yu, A review of integrated radiant heating/cooling with ventilation systems- Thermal comfort and indoor air quality, Energy Build. 223 (2020) 110094, <https://doi.org/10.1016/j.enbuild.2020.110094>.
- [23] W. Zhang, W. Zhang, K. Mizutani, H. Zhang, Decision-making analysis of ventilation strategies under complex situations: a numerical study, Build. Environ. 206 (2021) 108217, <https://doi.org/10.1016/j.buildenv.2021.108217>.
- [24] Z. Peng, et al., Practical indicators for risk of airborne transmission in shared indoor environments and their application to COVID-19 outbreaks, Environ. Sci. Technol. 56 (2) (2022) 1125–1137, <https://doi.org/10.1021/acs.est.1c06531>.
- [25] X. Zhao, Y. Yin, Hazards of pollutants and ventilation control strategy in industrial workshops: current state and future trend, Build. Environ. 251 (2024), <https://doi.org/10.1016/j.buildenv.2024.111229>.
- [26] Y. Lu, D. Niu, S. Zhang, H. Chang, Z. Lin, Ventilation indices for evaluation of airborne infection risk control performance of air distribution, Build. Environ. 222 (2022), <https://doi.org/10.1016/j.buildenv.2022.109440>.
- [27] Z. Shi, Z. Lu, Q. Chen, Indoor airflow and contaminant transport in a room with coupled displacement ventilation and passive-chilled-beam systems, Build. Environ. 161 (2019), <https://doi.org/10.1016/j.buildenv.2019.106244>.
- [28] X. Yuan, Q. Chen, L.R. Glicksman, A critical review of displacement ventilation, ASHRAE Transactions 104 (1) (1998) 78–90.
- [29] M. Sandberg, C. Blomqvist, Displacement ventilation systems in office rooms, Build. Eng. 95 (2) (1989) 1041–1049.
- [30] X. Yuan, Q. Chen, L.R. Glicksman, Performance evaluation and design guidelines for displacement ventilation, Build. Eng. 105 (1) (1999) 298–309.
- [31] F. Causone, F. Baldin, B.W. Olesen, S.P. Corgnati, Floor heating and cooling combined with displacement ventilation: possibilities and limitations, Energy Build. 42 (12) (2010) 2338–2352, <https://doi.org/10.1016/j.enbuild.2010.08.001>.
- [32] S. Javed, I.R. Ørnes, T.H. Dokka, M. Myrup, S.B. Holas, Evaluating the use of displacement ventilation for providing space heating in unoccupied periods using laboratory experiments, field tests and numerical simulations, Energies 14 (4) (2021), <https://doi.org/10.3390/en14040952>.
- [33] H. Brohus, P.V. Nielsen, Personal exposure in displacement ventilated rooms, Indoor Air 6 (3) (1996) 157–167, <https://doi.org/10.1111/j.1600-0668.1996.t01-1-00003.x>.
- [34] S. Mazumdar, Y. Yin, A. Guity, P. Marmion, B. Gulick, Q. Chen, Impact of moving objects on contaminant concentration distributions in an inpatient ward with displacement ventilation, HVAC&R Res. 16 (5) (2010) 545–563, <https://doi.org/10.1080/10789669.2010.10390921>.
- [35] R. Yang, C.S. Ng, K.L. Chong, R. Verzicco, D. Lohse, Do increased flow rates in displacement ventilation always lead to better results? J. Fluid Mech. 932 (2021) <https://doi.org/10.1017/jfm.2021.949>.
- [36] D. Licina, A. Melikov, C. Sekhar, K.W. Tham, Human convective boundary layer and its interaction with room ventilation flow, Indoor Air 25 (1) (2015) 21–35, <https://doi.org/10.1111/ina.12120>.
- [37] D. Licina, A. Melikov, J. Pantelic, C. Sekhar, K.W. Tham, Human convection flow in spaces with and without ventilation: personal exposure to floor-released particles and cough-released droplets, Indoor Air 25 (6) (2015) 672–682, <https://doi.org/10.1111/ina.12177>.
- [38] H. Qian, Y. Li, P.V. Nielsen, C.E. Hyldgaard, T.W. Wong, A.T. Chwang, Dispersion of exhaled droplet nuclei in a two-bed hospital ward with three different ventilation systems, Indoor Air 16 (2) (2006) 111–128, <https://doi.org/10.1111/j.1600-0668.2005.00407.x>.
- [39] W. Wu, Z. Lin, Experimental study of the influence of a moving manikin on temperature profile and carbon dioxide distribution under three air distribution methods, Build. Environ. 87 (2015) 142–153, <https://doi.org/10.1016/j.buildenv.2015.01.027>.
- [40] W. Wu, Z. Lin, An experimental study of the influence of a walking occupant on three air distribution methods, Build. Environ. 85 (2015) 211–219, <https://doi.org/10.1016/j.buildenv.2014.12.009>.
- [41] H. Yamasawa, T. Kobayashi, T. Yamanaka, N. Choi, M. Cehlin, A. Ameen, Applicability of displacement ventilation and impinging jet ventilation system to heating operation, Japan Architectural Review 4 (2) (2021) 403–416, <https://doi.org/10.1002/2475-8876.12220>.
- [42] ASHRAE, ASHRAE Position Document on Indoor Carbon Dioxide, 2022.
- [43] J. Kim, A. Tzempelikos, J.E. Braun, Energy savings potential of passive chilled beams vs air systems in various US climatic zones with different system configurations, Energy Build. 186 (2019) 244–260, <https://doi.org/10.1016/j.enbuild.2019.01.031>.
- [44] D.N. Wagner, A. Mathur, B.E. Boor, Spatial seated occupancy detection in offices with a chair-based temperature sensor array, Build. Environ. 187 (2021), <https://doi.org/10.1016/j.buildenv.2020.107360>.
- [45] W. Tian, A review of sensitivity analysis methods in building energy analysis, Renew. Sustain. Energy Rev. 20 (2013) 411–419, <https://doi.org/10.1016/j.rser.2012.12.014>.
- [46] S. Zhang, Y. Lu, D. Niu, Z. Lin, Energy performance index of air distribution: thermal utilization effectiveness, Appl. Energy 307 (2022) 118122, <https://doi.org/10.1016/j.apenergy.2021.118122>, 2022/02/01/.
- [47] G. Zheng, C. Shen, A. Melikov, X. Li, Improved performance of displacement ventilation by a pipe-embedded window, Build. Environ. 147 (2019) 1–10, <https://doi.org/10.1016/j.buildenv.2018.10.006>.
- [48] S. Liu, M. Koupryanov, D. Paskaruk, G. Fediuk, Q. Chen, Investigation of airborne particle exposure in an office with mixing and displacement ventilation, Sustain. Cities Soc. 79 (2022) 103718, <https://doi.org/10.1016/j.scs.2022.103718>.
- [49] G. Pei, D. Rim, S. Schiavon, M. Vannucci, Effect of sensor position on the performance of CO₂-based demand controlled ventilation, Energy Build. 202 (2019), <https://doi.org/10.1016/j.enbuild.2019.109358>.
- [50] N.M. Mateus, G. Carrilho da Graça, Simulated and measured performance of displacement ventilation systems in large rooms, Build. Environ. 114 (2017) 470–482, <https://doi.org/10.1016/j.buildenv.2017.01.002>.
- [51] R.K. Bhagat, P.F. Linden, Displacement ventilation: a viable ventilation strategy for makeshift hospitals and public buildings to contain COVID-19 and other airborne diseases, R. Soc. Open Sci. 7 (9) (2020) 200680, <https://doi.org/10.1098/rsos.200680>.
- [52] L. Feng, R. Li, Y. Wu, N. Gao, A zonal model to predict the vertical temperature distribution of displacement ventilation system during human movement, Build. Environ. 231 (2023), <https://doi.org/10.1016/j.buildenv.2023.110040>.
- [53] J. Ren, J. He, X. Kong, H. Li, Robustness of ventilation systems in the control of walking-induced indoor fluctuations: method development and case study, Build. Simulat. (2022) 1–16, <https://doi.org/10.1007/s12273-022-0888-x>.
- [54] M. Oladokun, Z. Lin, Dynamic sequential box modelling of inhalation exposure potential in multi-bed patient ward: Validation and baseline case studies, Build. Environ. 161 (2019), <https://doi.org/10.1016/j.buildenv.2019.106241>.
- [55] S. Yang, A. Muthalagu, V.G. Serrano, D. Licina, Human personal air pollution clouds in a naturally ventilated office during the COVID-19 pandemic, Build. Environ. 236 (2023) 110280, <https://doi.org/10.1016/j.buildenv.2023.110280>.
- [56] A. Ghahramani, et al., Personal CO₂ bubble: context-dependent variations and wearable sensors usability, J. Build. Eng. 22 (2019) 295–304, <https://doi.org/10.1016/j.jobe.2018.11.015>.